Journal of Machine Engineering, Vol. 16, No. 3, 2016

Received: *24 March 2016* / Accepted*: 05 August 2016* / Published online: *06 September 2016*

chatter,
cutting force,
modelling

Krzysztof JEMIELNIAK[1*]
Miroslaw NEJMAN[1]
Dominika SNIEGULSKA-GRADZKA[1]

IDENTIFICATION OF DYNAMIC CUTTING FORCE COEFFICIENTS BY DIRECT MEASUREMENT OF CUTTING FORCES DURING VIBRATORY CUTTING

This paper presents the methodology of measuring the instantaneous cutting forces during vibratory cutting. It is based on elastically supported dynamometer vibrating with the tool during chatter. Acceleration of the dynamometer measured simultaneously allows for evaluation and elimination of inertia forces acting on the oscillating dynamometer. Displacements of the dynamometer and the tool in the feed direction during orthogonal cutting are measured by the contactless inductive sensor. The measurements allow for determination of averaged or instantaneous dynamic cutting force coefficients and their dependence on cutting conditions.

1. INTRODUCTION

Avoiding self-excited vibrations is necessary condition for the proper machining process. Prediction of stability limit is based on dynamic characteristics of cutting process and machine tool system [1]. The latter is usually determined by applying the modal analysis. Characteristic of cutting process is the cutting force dependence on instantaneous values of the uncut chip thickness changing due to the relative displacement between the workpiece and the tool in a direction perpendicular to the cutting edge r_t, machined surface waviness left during the previous pass r_T and the velocity of these displacements r_t':

$$F_r = F_{rk}(h) + F_{rc}(r_t'), \qquad F_t = F_{tk}(h) + F_{tc}(r_t') \tag{1}$$

$$h = h_0 + h_d = h_0 - r_t + r_T \tag{2}$$

where F_{rk}, F_{tk} – stiffness components of the cutting forces, depending on relative tool-workpiece displacements, F_{rc}, F_{tc} – damping components of the cutting forces, depending on velocity of relative tool-workpiece vibrations r_t', h – uncut chip thickness, h_0 – static

[1] Department of Automation Machine Tools and Metal Cutting, Faculty of Production Engineering, Warsaw University of Technology, Poland
[*] E-mail: k.jemielniak@wip.pw.edu.pl

uncut chip thickness, h_d – dynamic component of h, $r_t = r(t)$ – inner modulation of h, $r_T = r(t\text{-}T)$ – outer modulation of h, v_c – cutting speed, T – tooth passing time interval.

Although relatively complex models of the cutting process characteristic (1) have been known for a long time, e.g. [6],[7],[16] the simple, linear Altintas model [1],[4], where the dynamic forces are proportional to the uncut chip thickness, is most often used:

$$F_r = k_r\, bh\,, \qquad F_t = k_t\, bh \tag{3}$$

where k_r, k_t – constant cutting coefficients, b – width of the cut.

The cutting coefficients are usually determined from steady state data [6],[7]. This solution is sufficiently accurate for turning, when the nominal uncut chip thickness h_0 is constant. However, in milling uncut chip thickness is inherently variable, sometimes from zero to the maximum. Therefore sometimes set of local models are used [12], covering the different cutting conditions, e.g. within a certain range of the uncut chip thickness.

Since the earliest works on chatter stability (e.g. [14]), the process damping was noticed as it has significant influence on stability, especially at lower cutting speeds [10]. However, it was usually ignored as there is no model or direct measurement method available to estimate process damping coefficients [5],[15]. Recently there have been many efforts to determine the process damping indirectly or by inverse fitting the damping coefficient value to stability limit. Sellmeier and Denkena [13] developed an analytical model based on the assumption that the damping force is proportional to the indented volume of the workpiece material by the chamfered flank face of the tool. The indented volume is dependent on the working clearance angle α_{oe} or inclination angle η of the vibrating tool path:

$$\alpha_{oe} = \alpha_o + \eta \ \approx\ \alpha_o + r_t'/v_c \tag{4}$$

Process damping coefficients were determined through a match of the experimentally determined stability chart with the theoretically calculated ones. Budak and Tunc [5] also analysed process damping assuming that it depends on the contact pressure and the volume of the deformed material under flank face, however they did not use artificial chamfered tools. They identified average process damping coefficient from the difference between the stability limits determined at low and high speeds. Kurata et al. [11] proposed damping coefficient identification from plunge turning tests, which created a continuous reduction of cutting speed. When chatter stopped at a critical cutting speed, the coefficient was estimated by inverse solution of stability limit.

Despite the fact that penetration of the tool into the wavy workpiece surface occurs only when the tool moves towards the workpiece ($r_t'<0$), in all these works the damping coefficient was averaged. That is the usual practice when the cutting process damping is taken into account in stability analysis [5],[11] and leads to the characteristic of the cutting process in the form:

$$F_r = b(k_r\, h + c_r\, r_t'), \qquad F_t = b(k_t\, h + c_t\, r_t') \tag{5}$$

where r_t'-vibration velocity in the uncut chip thickness direction, c_r, c_t – damping coefficients of the cutting forces.

An innovative idea was presented by Altintas et al. [2],[3] aiming at direct, simultaneous measurements of the tool displacement and cutting forces dynamic cutting tests. The fast tool servo was mounted on the turret of the machine and a three component load cell was integrated in the tool holder to measure the dynamic cutting forces. The dynamic cutting force coefficients were extracted using the least squares method applied to the frequency domain representation of measured forces. The authors did not explain how they eliminated inertia forces acting on the vibrating load cell.

This paper introduces an innovative methodology of direct measurement of dynamic cutting forces in vibratory cutting (during chatter). The methodology is based on the elastically supported dynamometer, which vibrates with the tool [9]. The initial results of its application in preliminary impact tests (without chatter) were presented in [8]. Here the full methodology and the example application for vibratory cutting are presented.

2. DIRECT CUTTING FORCE MEASUREMENT DURING CHATTER

The main idea of the new method of dynamic cutting force coefficients identification is a direct measurement of the cutting forces during actual chatter. That means that the cutting tool has to be rigidly fixed to the dynamometer supported by flexible elements. Thus the dynamometer directly measures the cutting forces acting on the tool under vibratory changes of uncut chip thickness and the tool geometry. The idea of the test stand is presented in Fig. 1. The measuring device consists of two plates (top and bottom) connected by two flat springs 2 mm thick. They ensure that the stiffness of the system in x is much lower than in other directions and the system can be considered as 1DOF.

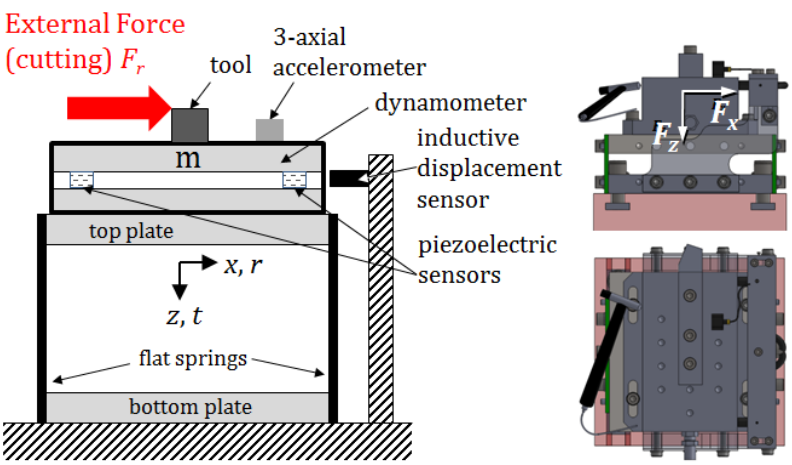

Fig. 1. The concept (left) and design (right) of the test rig for measurements of the dynamic components of the cutting forces [8]

The 3-axial dynamometer mounted on the top plate enables measurement of the feed force F_r and tangential force F_t acting on the tool fixed to the top surface of the dynamometer during orthogonal cutting. A 3-axial accelerometer is also fixed on the top of the dynamometer. A contactless inductive displacement sensor rigidly mounted to the base and is used for measuring the displacements of the dynamometer and the tool.

The dynamometer signals are proportional to the forces acting on the piezoelectric transducers. In a typical application when a dynamometer is rigidly mounted to the base (not moving) the output signal is proportional to the external force (e.g. cutting force). When the dynamometer vibrates, the transducers are affected by the inertial force proportional to the mass m of the upper part of the dynamometer and elements mounted on top of it and acceleration of the oscillatory motion. In such a case the dynamometer works exactly as an accelerometer. This inertial force adds to the external force resulting in a disturbance of the measured force F_x:

$$F_x = F_r + F_{xa} = F_r + m_x a; \qquad F_z = F_t + F_{za} = F_t + m_z a \tag{6}$$

where F_x, F_z – measured force in x, z direction, F_r, F_t - external force affecting on the dynamometer; F_{xa}, F_{za} - inertia force acting on the upper part of the dynamometer and items mounted on it, m_x, m_z - modal mass of the upper part of the dynamometers, a - acceleration of the dynamometer. To evaluate modal mass m the dynamometer is stimulated for free vibration by a hit with a modal hammer. After a short period of the hit the unloaded dynamometer registers only inertia forces ma. Thus after removing the initial part of the measured signal it can be correlated with the signal from the independent accelerometer. To take into account possible crosstalk between x and z axis signals, both forces and accelerations were measured simultaneously and the inertia forces were calculated using regression analysis from the equations:

$$F_{xa} = m_{xx}x'' + m_{zx}z'' \tag{7}$$
$$F_{za} = m_{xz}x'' + m_{zz}z'' \tag{8}$$

where, F_{xa} F_{za} – inertia force in the x and z direction equal to measured signals F_x and F_z after the hit, x”, z” – signals from accelerometer, m_{xx}, m_{zx}, m_{xz}, m_{zz} – modal mass coefficients.

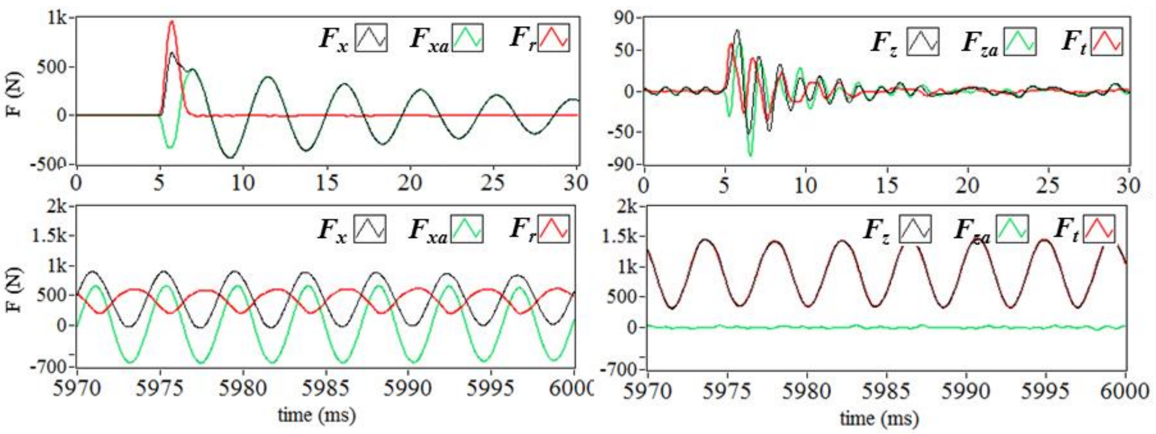

Fig. 2. The effect of elimination of inertial forces influence on F_r and F_t measurements after the modal hammer hit (upper row) and during chatter (lower row)

Fig. 2 shows the original signal from the dynamometer F_x, F_z, inertia forces F_{xa} and F_{za} and actual external forces F_r, F_t calculated with the formulas (6-8). The first row shows the forces measured after hit of the modal hammer and the second the forces registered during chatter.

3. EXPERIMENTAL SETUP

Fig. 3 presents the test rig mounted on the lathe, based on the concept presented in Fig. 1. The bottom plate of designed device is fixed onto T-slots of slide lathe. The test rig was equipped with Kistler 9257BA dynamometer, Kistler 8763A50 3-axis accelerometer and OT18 inductive displacement sensors and 3-axis accelerometer. Conventional TUD 100 lathe was used with a rotary encoder mounted on the spindle.

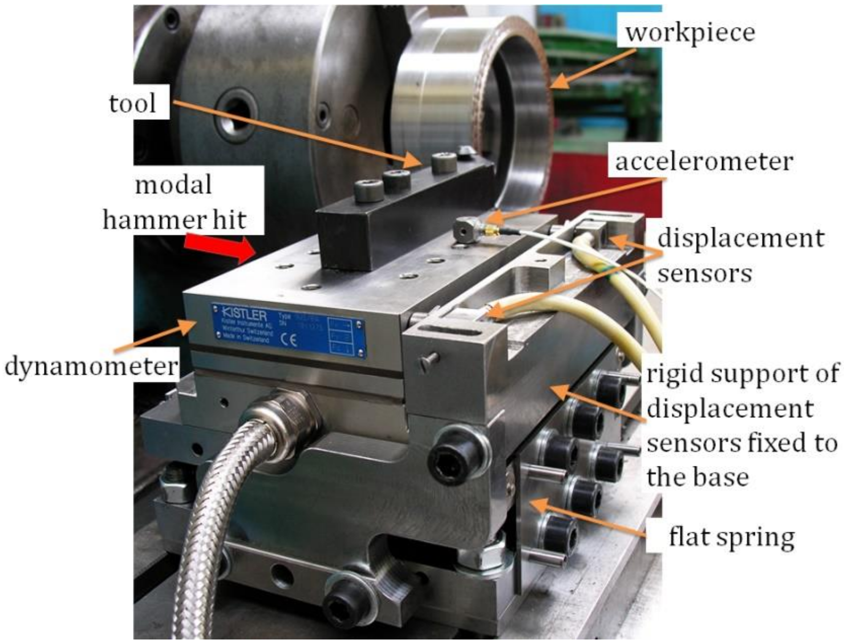

Fig. 3. Test rig mounted on the lathe

The workpiece was 125 mm diameter tube 2.5 mm thick made of S355J2H steel. The tool was CTGPR2525 turning tool with inserts TPGN 160304, grade 1025 (cemented carbide PVD coated with TiAlN layer) used for orthogonal cutting (without engagement of the nose). Tool geometry: κ_r=90° γ_o=5°, α_o=6°. The tool was kept sharp. All signals were registered using NI USB-6251 DAQ card with sampling rate 40kS/s. As the natural frequency of the dynamometer was ~1.7kHz, acceleration and force signals were 1500 Hz low-pass filtered. The encoder signals (150 pulses/rev) were converted into a ramp pattern from one pulse to another which allowed for precise determination of angular position of the workpiece, thus the identification of the tool displacement r_T exactly one revolution before actual r_t.

4. EXPERIMENTAL RESULTS AND DISCUSSION

Numerous orthogonal cutting tests were executed with depth of cut a_p=2.5mm, cutting speed v_c=15, 30, 60, 100, 120, 160, 200 and 240 m/min and feed f=0.08, 0.13 and 0.20 mm/rev. All measurements were performed after full development of chatter, when vibration amplitude stabilizes. Tests carried out at 15 and 30 m/min appeared to be stable, thus useless for the purpose of this investigation. Also only for cutting speed v_c=60 m/min the chatter occurred for all feeds. Therefore eight tests were selected for this presentation named after applied cutting speeds and feeds: v60f08, v60f13, v60f20, v100f08, v120f08, v160f08, v200f08, v240f08.

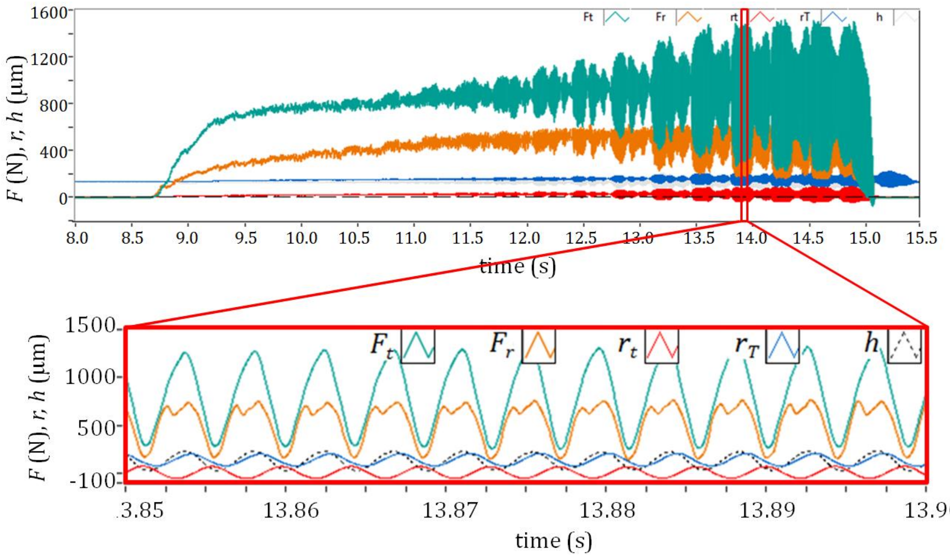

Fig. 4. Cutting forces and tool vibrations in test v60f13

In Fig. 4 measured cutting forces F_r and F_t together with actual displacements of the tool r_t, chatter marks r_T+h_0 and uncut chip thickness h obtained in test v60f13 were presented. While the tangential force F_t looks approximately directly related to uncut chip thickness h the feed force shows eminent grows when the vibration speed r_t'<0. This suggests expected influence of cutting process damping. To examine this phenomenon it was decided to separate the influence of the uncut chip thickness h and vibration speed r_t' on the feed force by simple statistic polynomial regression. The measurements might be subject of any sophisticated, physical modelling of dynamic cutting coefficients. Here, just for example several statistical models were tested and three of them appeared to be worth attention:

model 1, linear generally used in stability analysis:

$$F_r = b(F_0 + k_{r1}h) + bc_{r1}r_t' = F_{rk} + F_{rc} \tag{9}$$

model 2, with linear stiffness and nonlinear damping force:

$$F_r = b(F_0 + k_{r1}h) + b\left(c_{r1}r_t' + c_{r2}{r_t'}^2\right) = F_{rk} + F_{rc} \tag{10}$$

model 3, with both stiffness and damping force nonlinear:

$$F_r = b(F_0 + k_{r1}h + k_{r2}h^2) + b\left(c_{r1}r_t' + c_{r2}{r_t'}^2\right) = F_{rk} + F_{rc} \tag{11}$$

where F_0, k_{r1}, k_{r2}, c_{r1}, c_{r2} – cutting force coefficients.

Results are presented in Fig. 5 where the F_r force measured during test v60f13 with black lines. The cutting stiffness forces are marked with blue lines, while the damping forces are green. The red lines are the F_r force modelled using equations (9-11). Below the tool vibrations r_t , h_0+r_T and h are presented. It is evident, that the first, simplest, linear model averages the actual cutting force course neglecting characteristic growth of the force during the tool "diving" into the workpiece material. The second model provides better results, showing, that the damping force acts mainly when the tool moves towards the workpiece, while is close to zero during opposite movement. The third model gives even better agreement between the measured (black line) and modelled (red line) values of the F_r. The numerical values of the cutting force coefficients obtained in all three models with the correlation coefficients are presented in Table 1.

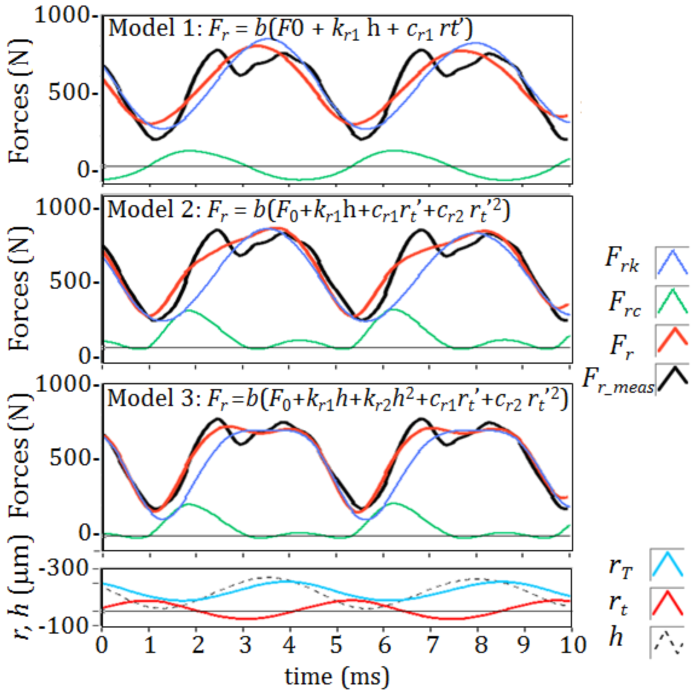

Fig. 5. Statistical modelling of the feed force in test v60f13

Table 1 Cutting force coefficients obtained in test v60f13

Model	F_{r0} N	k_{r1} N/mm^2	k_{r2} N/mm^3	c_{r1} Ns/mm^2	c_{r2} Ns^2/mm^3	corr. coeff
1	75.66	1098		-0.424		0.904
2	45.12	1116		-0.373	0.067	0.944
3	-6.984	2482	-5411	-0.370	0.052	0.983

Polynomials of higher degree and influence of the tool acceleration r_t'' were also tested, but they did not provide better results. For tangential cutting force the second model appeared to be sufficient.

In Fig. 6 results of all tests performed with the cutting speed v_c=60m/min are presented for both cutting force components – F_t model 2, F_r model 3. It is worth noticing, that only in test v60f08, when the nominal uncut chip thickness was the smallest (h_0=0.08 mm) tool jumped out of the material, which was one of the reasons of the chatter amplitude stabilization. The measured forces did not drop to zero when h=0 because of mentioned low pass filtering of the signals.

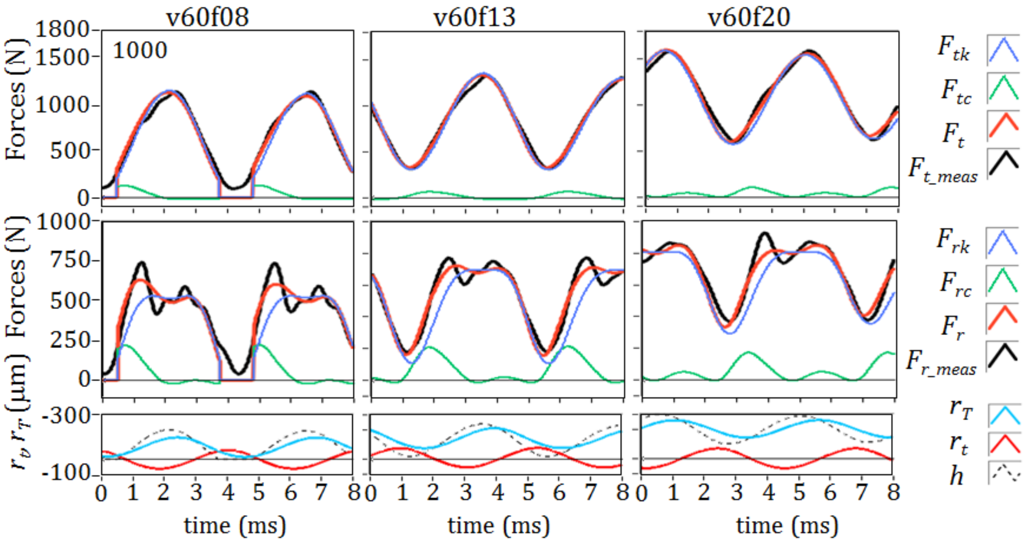

Fig. 6. Statistical modelling of the cutting forces for cutting speed vc=60m/min

The second reason of the amplitude stabilization was damping force acting on the flank surface of the tool, mainly when r_t'<0. This damping caused the chatter amplitude stabilization for higher feeds. It is also worth mentioning that damping component of the F_t force is much smaller than those of F_r force, even though F_r is double F_r. All obtained cutting force coefficients for v_c=60 m/min are presented in Table 2. For cutting speeds higher than v_c=60m/min for both cutting forces F_r and F_t the second model appeared to be adequate enough.

Table 2 Cutting force coefficients obtained for vc=60m/min (*j*=*t* or *r*)

test		F_{j0} N	k_{j1} N/mm^2	k_{j2} N/mm^3	c_{j1} Ns/mm^2	c_{j2} Ns/mm^3	corr. coef.
v60f08	F_t	81.16	1907		-5.306	0.663	0.986
	F_r	55.01	1894	-5720	-7.619	1.513	0,952
v60f13	F_t	80.23	1935		-3,062	0.262	0,993
	F_r	-6.98	2482	-5411	-6.526	1.623	0.983
v60f20	F_t	22.41	2046		-1.757	0.967	0.989
	F_r	-173.3	3503	-6190	-3.820	1.501	0.967

Fig. 7 presents results of feed force coefficient modelling for all eight experiments. Fig. 7a shows differences between the measured values of the feed force (F_{r_meas}) and modelled damping force F_{rc}, which gives approximately measured stiffness feed force. Below (Fig. 7b) modelled stiffness components of the feed forces are presented. It can be noticed, that for v_c>60m/min the linear model of the cutting force coefficient k_{r1} is adequate enough, and its value diminishes with the rising cutting speed.

In Fig. 7c differences between the measured values of the feed force (F_{r_meas}) and modelled stiffness force F_{rk}, this gives approximately measured damping feed force. Below (Fig. 7d) modelled damping components of the feed forces are shown. Dependence of the feed force damping on the vibration speed r_t' looks rather scattered. However when instead of this speed the inclination angle η or the working clearance angle α_{oe} are considered as independent variable, the feed damping force appears to be repeatable - see Fig. 7e and 7f. It is also worth noticing, that in any circumstances, any test the working clearance angle did was not below 0° (inclination angle η>-6°) due to damping force rising strongly when α_{oe} approached zero.

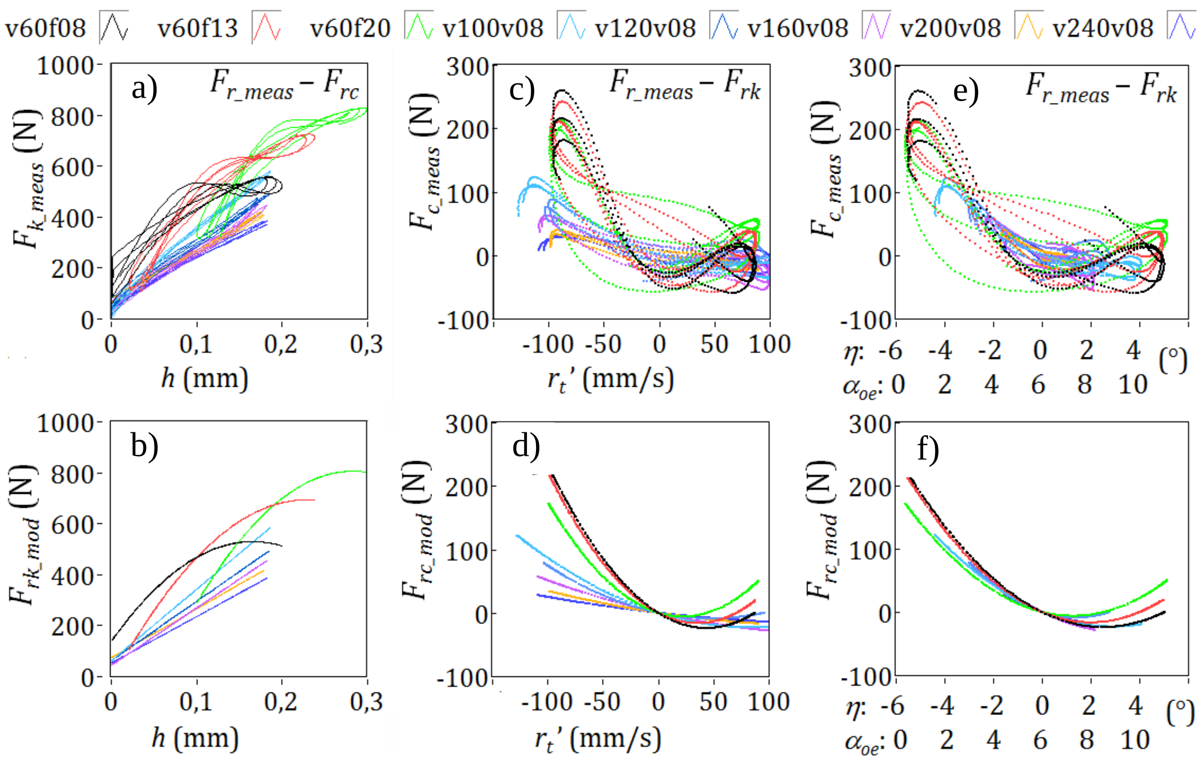

Fig. 7. Statistical modelling of the feed force coefficients in all tests

Tangential stiffness force coefficients appeared to be much simpler, linear, and not dependent on feed or cutting speed. Tangential damping force was scattered, but much smaller than for feed direction.

As in stability analysis usually linear model is used, in table the linear cutting force coefficients obtained in all tests are summarized.

Table 3 Linear cutting force coefficients obtained in all tests

test	F_{r0} N	k_{r1} N/mm^2	c_{r1} Ns/mm^2	F_{t0} N	k_{t1} N/mm^2	c_{t1} Ns/mm^2
v60f08	132.5	570	-0.422	97.0	1855	-0.299
v60f13	75.7	1098	-0.424	84.0	1932	-0.180
v60f20	81.4	974	-0.200	38.2	2038	-0.111
v100f08	37.5	1096	-0.207	39.6	1936	-0.140
v120f08	34.8	913	-0.144	50.3	1720	-0.066
v160f08	20.2	902	-0.156	22.1	1793	-0.175
v200f08	31.1	768	-0.104	21.6	1679	-0.102
v240f08	22.3	732	-0.077	16.6	1636	-0.018

5. SUMMARY

A new methodology of direct measurement of cutting forces during vibratory cutting presented in this paper enables much more accurate evaluation of cutting force dependence on instantaneous cutting conditions. The key issue solved by the methodology is the identification and elimination of inertia force acting on the dynamometer, which is higher than the dynamic component of cutting force. It can be applied for simple experimental determination of linear cutting force coefficients necessary for analytical stability analysis (as presented in Table 3), or for verification of models of cutting process damping, and for developing more accurate formulas describing these coefficients which can be applied for numerical simulation of self excited vibrations.

ACKNOWLEDGMENTS

Financial support of Structural Funds in the Operational Programme - Innovative Economy (IE OP) financed from the European Regional Development Fund - Project "Modern material technologies in aerospace industry", Nr POIG.01.01.02-00-015/08-00 is gratefully acknowledged.

REFERENCES

[1] ALTINTAS Y., 2000, *Manufacturing automation*, Cambridge University Press.
[2] ALTINTAS Y., EYNIAN M., ONOZUKA H., 2008, *Identification of dynamic cutting force coefficients and chatter stability with process damping*, CIRP Annals - Manufacturing Technology, 57, 371-374.
[3] ALTINTAS Y., KILIC Z.M., 2013, *Generalized dynamic model of metal cutting operations*, CIRP Annals-Manufacturing Technology, 62, 47-50.
[4] BUDAK E., ALTINTAS Y., ARMAREGO E.J.A, 1996, *Prediction of milling force coefficients from orthogonal cutting data*, Journal of Manufacturing Science and Engineering, 118, 216-224.
[5] BUDAK E., TUNC L.T., 2010, *Identification and modeling of process damping in turning and milling using a new approach*, CIRP Annals - Manufacturing Technology, 59, 403-408.
[6] DAS M.K., TOBIAS S.A., 1967, *The relation between the static and the dynamic cutting of metals*, Int. J. Mach. Tool Des. Res., 7, 63-89.
[7] JEMIELNIAK K., 1992, *Modelling of dynamic cutting coefficients in three - dimensional cutting*, Int. J. Mach. Tools Manufact, 32/4, 509-519.
[8] JEMIELNIAK K., NEJMAN M., ŚNIEGULSKA-GRĄDZKA D., 2013, *New method of dynamic cutting force coefficients determination*, Proc. of the International Conference on Advanced Manufacturing Engineering and Technologies, 1, 159-166.

[9] JEMIELNIAK K., NEJMAN M., ŚNIEGULSKA-GRĄDZKA D., WYPYSIŃSKI R., 2012, *Device for dynamic components of cutting force measurement*, Patent P-398818, April 15.
[10] KEGG R.L., 1969, *Chatter behavior at low cutting speeds*, CIRP Annals, 17, 97-106.
[11] KURATA Y., MERDOL S.D., ALTINTAS Y., SUZUKI N., SHAMOTO E., 2010, *Chatter stability in turning with in process identified process damping,* Journal of Advanced Mechanical Design, Systems and Manufacturing, 4/6, 1107-1118.
[12] PARIS H., BRISSAUD D., GOUSKOV A., 2007, *A more realistic cutting force model at uncut chip thickness close to zero,* CIRP Annals - Manufacturing Technology, 56, 415-418.
[13] SELLMEIER V., DENKENA B., 2012, *High speed process damping in milling*, CIRP Journal of Manufacturing Science and Technology, 5, 8-19.
[14] TOBIAS A., FISHWICK W., 1958, *Chatter of lathe tools under orthogonal cutting conditions*, Trans of ASME:B, 1079-1088.
[15] TUNC L.T., BUDAK E., 2012, *Effect of cutting conditions and tool geometry on process damping in machining*, International Journal of Machine Tools & Manufacture, 57, 10-19.
[16] BACH P., POLACEK M., CHVOJKA P., BURIAN D., DROBILEK J., 2014, *A method of identification of complex cutting forces acting in unstable cutting process*, Journal of Machine Engineering, 14/4, 18-28.